Cell, Vol. 114, 285–297, August 8, 2003, Copyright ©2003 by Cell Press

A *C. elegans* Sperm TRP Protein Required for Sperm-Egg Interactions during Fertilization

X.-Z. Shawn Xu and Paul W. Sternberg*
Howard Hughes Medical Institute and Division of Biology
California Institute of Technology
Pasadena, California 91125

Summary

Fertilization, a critical step in animal reproduction, is triggered by a series of specialized sperm-egg interactions. However, the molecular mechanisms underlying fertilization are not well understood. Here, we identify a sperm-enriched *C. elegans* TRPC homolog, TRP-3. Mutations in *trp-3* lead to sterility in both hermaphrodites and males due to a defect in their sperm. *trp-3* mutant sperm are motile, but fail to fertilize oocytes after gamete contact. TRP-3 is initially localized in intracellular vesicles, and then translocates to the plasma membrane during sperm activation. This translocation coincides with a marked increase in store-operated calcium entry, providing an in vivo mechanism for the regulation of TRP-3 activity. As *C. elegans* oocytes lack egg coats, our data suggest that some TRPC family channels might function to mediate calcium influx during sperm-egg plasma membrane interactions leading to fertilization.

Introduction

The TRP (transient receptor potential) superfamily of cation channels comprises three primary subfamilies, TRPC (TRP-canonical), TRPV (TRP-vanilloid), and TRPM (TRP-melastatin), which are conserved from worms to humans (Harteneck et al., 2000; Montell et al., 2002b). Studies in mice and *C. elegans* have demonstrated that members of the TRPV subfamily are involved in thermosensation and nociception as they are activated by temperature and various noxious stimuli (reviewed in Caterina and Julius, 2001; Montell et al., 2002a; Tobin et al., 2002). TRPM channels have been implicated in a wide spectrum of physiological processes ranging from cold sensation to cell viability, and are regulated by diverse mechanisms including cold temperature, ADP-ribose, H_2O_2, and intracellular Ca^{2+} and Mg^{2+} (reviewed in Montell et al., 2002a).

The TRPCs are the founding members of the TRP superfamily; nevertheless, their modes of activation and functions remain enigmatic. While stimulation of phospholipase C (PLC) seems to precede TRPC activation, the precise mechanisms leading to TRPC activation remain controversial (Montell et al., 2002a). Furthermore, despite the wide expression of TRPCs in nearly every cell type, the in vivo functions of TRPCs are poorly understood. One notable exception appears to be in sensory neurons, where TRPCs are required for visual transduction *in Drosophila* and for pheromone detection in mice (reviewed in Montell et al., 2002a).

Fertilization is triggered by a series of specialized sperm-egg interactions including gamete recognition, binding, and fusion (reviewed in Primakoff and Myles, 2002; Wassarman, 1999). Several molecules involved in these processes have been identified in mice. Examples include ZP3, the egg ligand for sperm-egg recognition, and fertilin and CD9, both of which have been implicated in sperm-egg binding and/or fusion (reviewed in Primakoff and Myles, 2002; Wassarman, 1999). Nevertheless, the molecular mechanisms underlying sperm-egg interactions are not well understood. Recently, *C. elegans* has emerged as a genetic model for the study of fertilization (reviewed in Singson, 2001). Nematode sperm, despite their morphological differences from mammalian sperm, have basic functions common to all sperm, including spermatogenesis, sperm activation (spermiogenesis), motility, gamete recognition/adhesion, and gamete fusion (L'Hernault, 1997; Singson, 2001). Several mutants that are specifically defective in fertilization have been isolated (Singson, 2001), including *spe-9*, which encodes a gene with EGF-like repeats that may act as a sperm ligand for gamete recognition and/or binding (Singson et al., 1998).

To explore the biological functions of TRPC proteins, we isolated mutations in the sperm-enriched *C. elegans TRPC* homolog, *trp-3*. *trp-3* mutant animals are nearly sterile due to the failure of their sperm to initiate fertilization after gamete contact. TRP-3 is localized to intracellular vesicles in spermatids and translocates to the plasma membrane during sperm activation. Since this translocation is accompanied by a marked increase in store-operated Ca^{++} entry, this observation provides a mechanism for the regulation of TRP-3 activity in vivo.

Results

Isolation of *trp-3* Mutants

The *C. elegans* genome encodes three TRPC homologs that we refer to as TRP-1, TRP-2 and TRP-3 (previously CeSTRPC1 [ZC21.2], CeSTRPC2 [R06B10.4] and CeSTRPC3 [K01A11.4 and SPE-41], respectively) (Harteneck et al., 2000; Montell et al., 2002b; wormbase.org), each of which bears the hallmarks of the TRPC family. These include 2 to 4 ankyrin repeats and a coiled-coil domain in the amino-terminus, six putative transmembrane domains, and a TRP domain in the proximal carboxyl-terminal region (Harteneck et al., 2000) (Figure 1A). We isolated two *trp-3* alleles by screening for mutagen-induced deletions in *trp-3* (Figures 1B and 1C). *trp-3*(*sy693*) deleted an ~2.2 kb genomic fragment encoding two-thirds of the N terminus and four transmembrane domains, and *trp-3*(*sy694*) removed a 700 bp segment that included the coding region for the first transmembrane domain (Figures 1B and 1C). Primers specific for the wild-type allele did not yield any PCR product from DNA isolated from *trp-3* homozygotes, excluding the presence of a duplicated *trp-3* gene that might have

*Correspondence: pws@caltech.edu

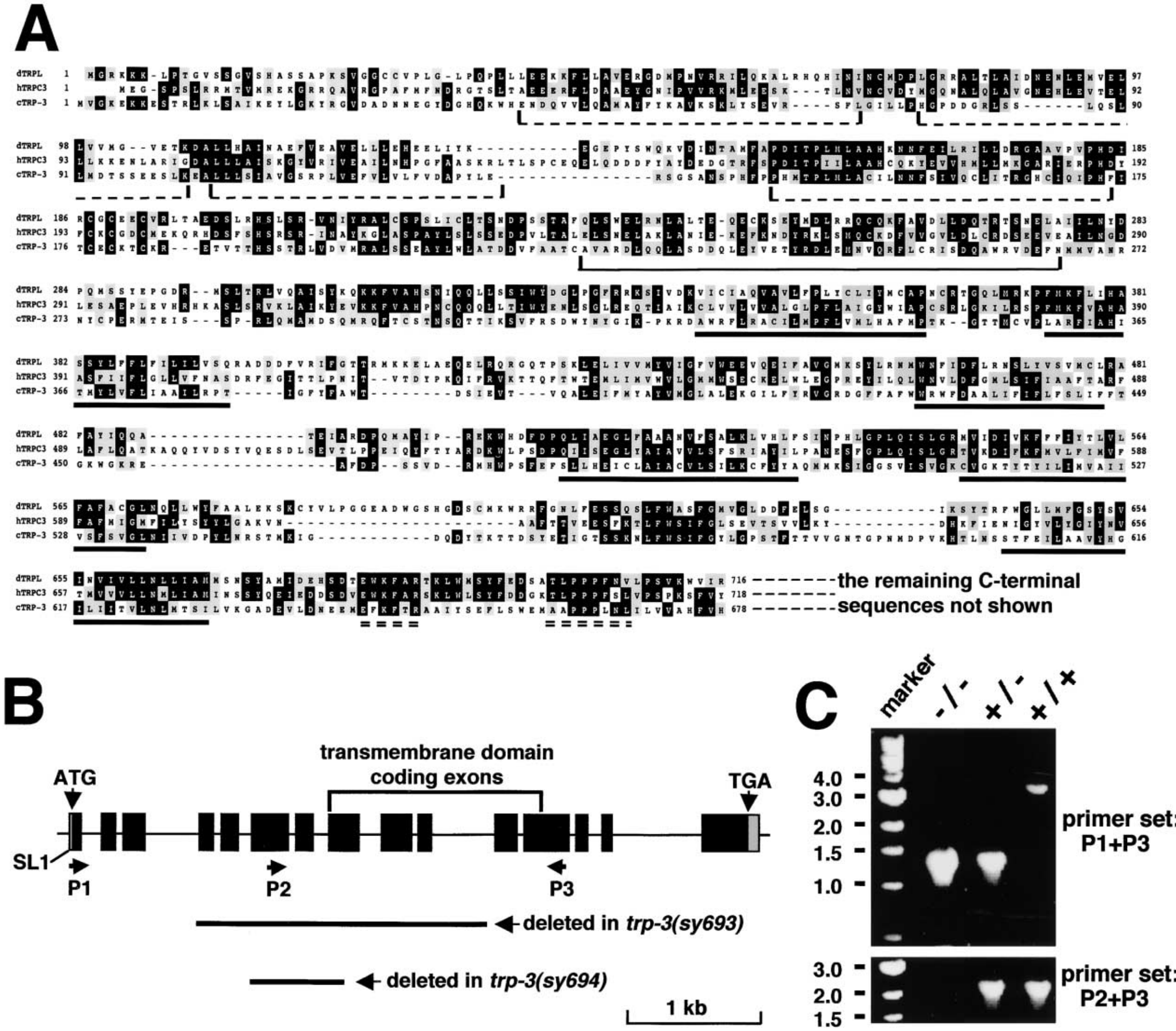

Figure 1. The *trp-3* Gene and Protein

(A) Alignment of *C. elegans* TRP-3 (cTRP-3), human TRPC3 (hTRPC3), and *Drosophila* TRPL (dTRPL). The underlying dashed brackets indicate ankyrin repeats; the underlying solid bracket indicates the coiled-coil domain. The six putative transmembrane domains are indicated by underlying solid lines. The two dotted lines indicate the TRP domain.

(B) *trp-3* genomic structure and *trp-3* mutations. The position for the *trans*-spliced leader (SL1) is indicated. The two solid lines underneath indicate the sequences that are deleted in *trp-3*(*sy693*) and *trp-3*(*sy694*), respectively. The positions for the primers used in PCR amplications in (C) are indicated and labeled P1, P2, and P3.

(C) PCR characterization of the *trp-3*(*sy693*) deletion mutant. The top panel shows the PCR products amplified by P1 and P3. No wild-type band was amplified in heterozygotes since the shorter mutant PCR fragment was highly favored. Shown in the bottom panel are the PCR fragments amplified by P2 and P3. No product was amplified in *trp-3*(*sy693*) homozygotes because of the deletion of the primer sequence of P2 in this mutant. Data for *trp-3*(*sy694*) not shown.

arisen during mutagenesis (Figure 1C). As transmembrane domains are generally required for ion channel function, both *sy693* and *sy694* should be null alleles.

trp-3 Mutants Are Infertile

Both *trp-3* mutants were nearly sterile with an average fertility of ~5% of wild-type hermaphrodites (Figure 2A; average brood size: 285.2 in wild-type versus 13.5 in *trp-3*). *trp-3*(*sy693*)/*trp-3*(*sy694*) trans-heterozygotes exhibited the same sterile phenotype as single mutants (Figure 2A), excluding the possibility that sterility was caused by a background mutation. Moreover, a transgene containing a cosmid that included the entire *trp-3* locus rescued the sterility, further demonstrating that *trp-3* was the gene responsible for the sterile phenotype (Figure 2A). *trp-3* was recessive since heterozygous hermaphrodites were fertile (Figure 2A).

In hermaphrodites, oocytes mature in the gonad in an assembly-line fashion and are then ovulated into the spermatheca, where sperm are stored and fertilization takes place (McCarter et al., 1999). Subsequently, fertilized oocytes exit the spermatheca and enter the uterus

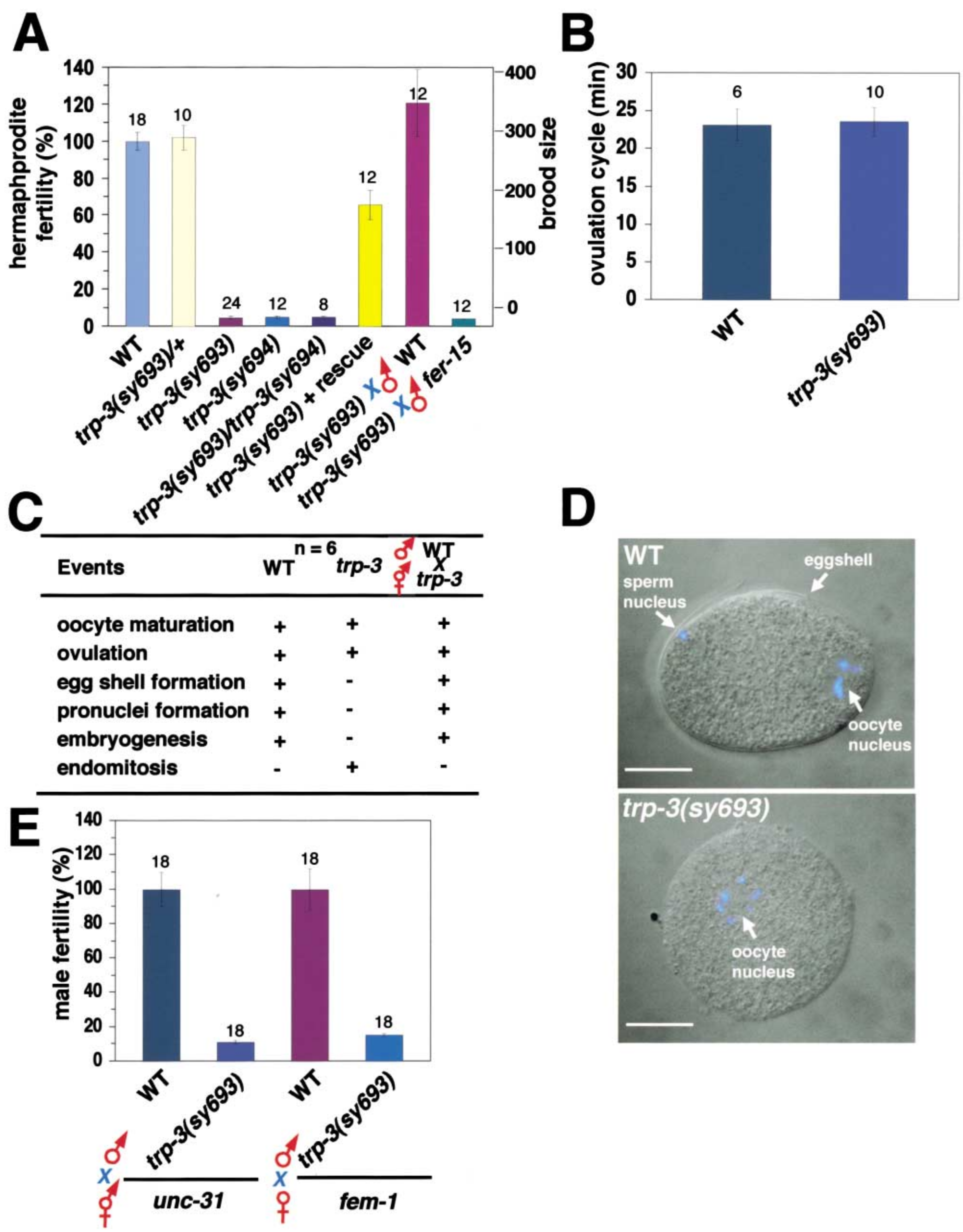

Figure 2. *trp-3* Mutants Are Sterile Due to a Defect in Sperm

(A) *trp-3* hermaphrodite mutants are nearly sterile. All the genotypes carry *him-5*(*e1490*). The Y-axis to the left indicates relative hermaphrodite fertility, while the Y-axis to the right indicates absolute brood size. The error bars indicate SEM. The transgene restored fertility to 67% of wild-type. The incomplete rescue may be due to low levels of transgene expression in the germ-line (Kelly and Fire, 1998).

(B) The ovulation cycle in *trp-3*(*sy693*) is normal.

(C) A summary of events prior to and surrounding fertilization. Events indistinguishable from wild-type are indicated as "+", whereas "−" indicates that the event did not occur.

(D) Oocytes are not fertilized in *trp-3*(*sy693*) animals. Shown are merged DIC (gray) and DAPI staining (blue) images. The positions of the eggshell, sperm, and oocyte nucleus are indicated by arrows. Scale bar = 10 μm.

(E) *trp-3*(*sy693*) males are nearly sterile. Wild-type or *trp-3*(*sy693*) males were crossed to *unc-31*(*e169*) hermaphrodites at 20°C or to *fem-1*(*hc17*) females at 25°C (*hc17* causes hermaphrodites to become females at 25°C). The total number of cross-progeny from *unc-31* or *fem-1* was counted. The mean numbers calculated from the crosses using wild-type males were normalized to 100%.

where embryogenesis begins. Defects in ovulation, oocytes, sperm, or embryogenesis all reduce brood size. *trp-3* sterility could arise from defects in any of these steps.

We found no obvious differences between the ovulation cycles of wild-type and *trp-3*(*sy693*) hermaphrodites (Figures 2B and 2C). Prior to ovulation, the oocytes in *trp-3*(*sy693*) hermaphrodite gonads underwent normal cycles of maturation, including the disappearance of the nucleolus, distal nuclear migration, and nuclear membrane breakdown (Figure 2C). These observations suggest that *trp-3* sterility is not due to defects in ovulation or oocyte differentiation, consistent with the absence of TRP-3 protein expression in oocytes (see below).

We next asked whether fertilization occurs in *trp-3* mutants. Eggshell formation, one of the first events following fertilization, was not observed in *trp-3*(*sy693*) mutants (Figure 2C), nor was pronuclei-formation or pronuclei-fusion detected in *trp-3*(*sy693*) oocytes that had exited from the spermatheca (Figure 2C). Consequently, these oocytes did not undergo cell division, but eventually entered endomitosis, in which DNA replication occurs without cytokinesis (McCarter et al., 1999) (Figure 2C).

The observations that the oocytes in *trp-3*(*sy693*) hermaphrodites did not form eggshells, failed to enter embryogenesis, and underwent endomitosis strongly suggest that they were not fertilized. However, these observations can also be explained by a defect in egg-activation following fertilization. Therefore, it remains possible that *trp-3*(*sy693*) sperm can fertilize oocytes, but that the fertilized oocytes are not activated to initiate embryogenesis. For example, *spe-11* encodes a sperm-supplied factor that is deposited into oocytes during fertilization and is required for triggering egg activation (Browning and Strome, 1996). To determine whether *trp-3*(*sy693*) sperm can fertilize oocytes, we stained eggs dissected from *trp-3*(*sy693*) uteri with DAPI. While a newly-entered sperm nucleus is clearly visible on the opposite side of the oocyte nucleus in wild-type embryos (Figure 2D, top, n = 9), no such sperm nucleus was detected in *trp-3*(*sy693*) oocytes (Figure 2D, bottom, n = 12), nor was an eggshell present in these oocytes (Figure 2D, bottom, n = 12). As polar bodies were not detected in *trp-3*(*sy693*) oocytes, it is unlikely that they completed meiosis (Figure 2D, bottom). We conclude that the ooctyes in *trp-3* mutants are not fertilized.

trp-3 Sperm Are Defective

The lack of gross abnormalities in ovulation or oocyte maturation, and the observation that fertilization does not take place in *trp-3* mutants suggest that the *trp-3* sperm might be responsible for the sterile phenotype. If so, then providing the mutant hermaphrodites with wild-type sperm should rescue the sterility. We therefore mated wild-type males into *trp-3*(*sy693*) hermaphrodites. This mating rescued the *trp-3*(*sy693*) fertility defect (Figure 2A). To ensure that sperm per se were responsible for the rescue, rather than a component of seminal fluid, we mated *fer-15*(*hc15*) males, which only produce nonfunctional sperm (L'Hernault et al., 1988), to *trp-3*(*sy693*) hermaphrodites. This mating failed to rescue the fertility defect (Figure 2A). Mating of wild-type males to *trp-3*(*sy693*) hermaphrodites also rescued the defects in eggshell formation, pronuclei formation and fusion, and embryogenesis/endomitosis (Figure 2C, n = 10). We also found that *trp-3*(*sy693*) males were nearly sterile (Figure 2E), and did not exhibit any gross abnormalities in mating behavior (n = 8). Taken together, we conclude that the *trp-3* sterility results from a defect in the sperm.

The TRP-3 Protein Is Highly Enriched in Sperm

We raised antisera against TRP-3 and found that the affinity-purified TRP-3 antibodies detected a strong signal in hermaphrodite sperm, but no other cell types (Figures 3A–3D). This finding is consistent with a genome-wide microarray study suggesting that the *trp-3* mRNA is enriched in sperm (Reinke et al., 2000). No TRP-3 expression was found in *trp-3*(*sy693*) mutants (Figures 3E–3H), indicating that the antibodies were specific. The absence of TRP-3 protein in *trp-3* mutants was not due to the absence of sperm because sperm nuclei were clearly visible in *trp-3* spermathecae (Figures 3F and 3G). Indeed, the number of sperm in *trp-3* and wild-type hermaphrodites was similar (158 ± 11 per spermatheca in *trp-3*, n = 12; 163 ± 15 in wild-type, n = 10). The TRP-3 expression pattern is consistent with the sperm defect observed in *trp-3* mutants.

trp-3(*sy693*) Sperm Are Motile, but Defective in Fertilization

Several different defects could impair the ability of sperm to fertilize oocytes. Developmental defects in spermatogenesis and/or sperm activation (spermiogenesis) often lead to the failure of spermatogenic cells or spermatids to develop into mature sperm (L'Hernault, 1997). Sperm motility is required for both male and hermaphrodite sperm to fertilize oocytes. Also, sperm displaying normal development and motility might fail to fertilize oocytes due to defects in gamete recognition, binding, and/or fusion (Singson, 2001).

To distinguish among these possibilities, we first examined whether *trp-3*(*sy693*) sperm were blocked at any developmental stage. The morphology of mature sperm (spermatozoa) differ from spermatids and spermatocytes in that they bear a pseudopod with villar projections on the surface (Singson, 2001). Dissected *trp-3*(*sy693*) hermaphrodite sperm were morphologically indistinguishable from wild-type sperm (Figures 4A–4C). Activated male-derived mature *trp-3* sperm also exhibited wild-type morphology (Figures 4D and 4E). *trp-3* sperm were motile in vitro (Figure 4F, n = 10), and displayed similar mean velocity to wild-type sperm on glass slides (26.1 ± 7.1 μm/min, n = 10 for *trp-3*; 28.5 ± 8.2 μm/min, n = 10 for wild-type; $p = 0.32$).

Sperm motility in vivo and in vitro are different in that sperm exhibit directional movement toward the spermatheca in vivo, rather than the random movement observed in vitro. To determine whether *trp-3* sperm are motile in vivo, we used a female strain, *fem-1*(*hc17*), that does not produce endogenous sperm (Spence et al., 1990). We reasoned that if *trp-3* sperm are motile in vivo, then we would expect to find *trp-3* sperm in *fem-1* spermathecae after mating *trp-3* males with *fem-1* females. Indeed, many *trp-3*(*sy693*) sperm reached the *fem-1*(*hc17*) spermatheca after mating (Figure 4G). Furthermore, *trp-3*(*sy693*) sperm readily surrounded the oocyte in the spermatheca (Figure 4H), indicating that *trp-3*(*sy693*) sperm were able to make contact with the oocyte. As a control, immotile sperm such as those from the spermiogenesis-defective *fer-1*(*hc1*) and *fer-15*(*hc15*) strains (L'Hernault et al., 1988) failed to reach the *fem-1*(*hc17*) spermatheca after mating (Figure 4I). No abnormality in male mating behavior was detected

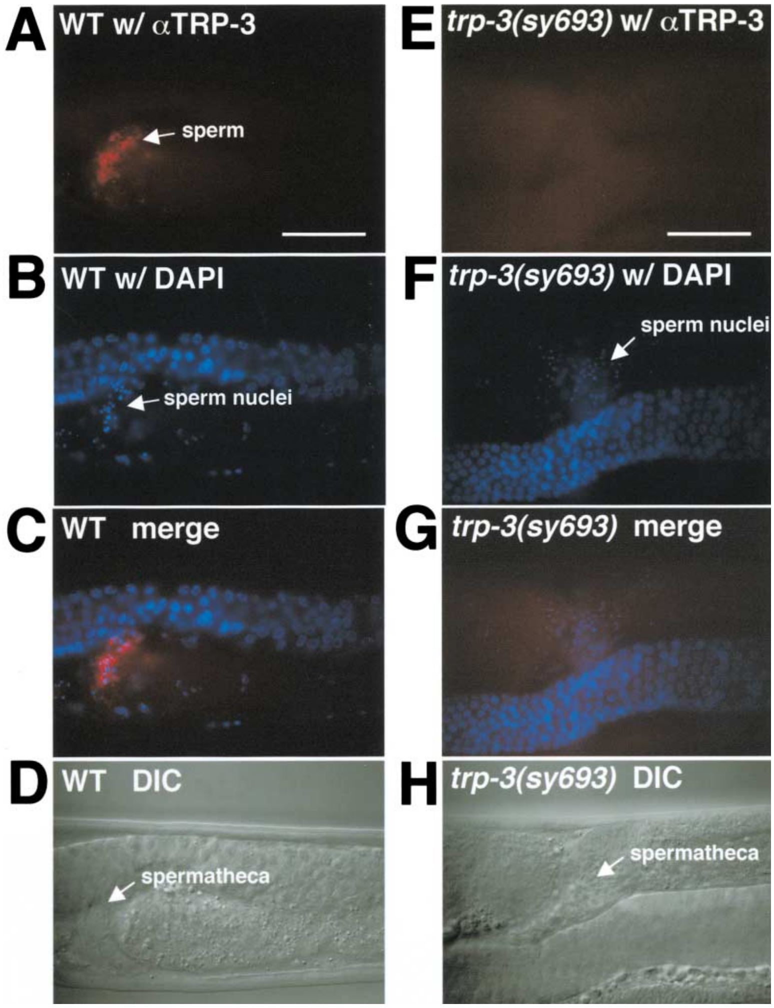

Figure 3. The TRP-3 Protein Is Highly Enriched in Sperm

(A–H) An affinity-purified antibody against TRP-3 specifically stains sperm in wild-type hermaphrodites. Scale bar = 10 μm.

(A) An immunofluorescence image of anti-TRP3 staining of a wild-type hermaphrodite.

(B) The same animal in (A) stained with DAPI.

(C) A superimposed image of (A) and (B).

(D) A DIC image of the same animal in (A–C).

(E–H) The TRP-3 antibody is specific.

(E) The TRP-3 antibody does not detect a signal in *trp-3*(*sy693*) mutants.

(F) A DAPI image of the same animal shown in (E).

(G) A superimposed image of (E) and (F).

(H) A DIC image of the same animal shown in (E–G).

in either *fer-1*(*hc1*) or *fer-15*(*hc15*) (n = 8). Thus, *trp-3*(*sy693*) sperm are motile in vivo and are capable of contacting oocytes.

It might be argued that since *trp-3*(*sy693*) males retain residual fertility, those *trp-3*(*sy693*) sperm that reached the *fem-1*(*hc17*) spermatheca after mating might represent the small population of functional *trp-3* sperm. However, each *fem-1*(*hc17*) spermatheca housed an average of 145 ± 41 *trp-3*(*sy693*) sperm (n = 12), nearly ten times that which would be expected based on the residual fertility in *trp-3*(*sy693*) males. Thus, the residual fertility in *trp-3* males is far from sufficient to account for the number of *trp-3* sperm present in the *fem-1*(*hc1*) spermatheca.

To provide functional evidence that *trp-3* sperm were motile, we performed a sperm competition assay. Although hermaphrodites carry endogenous sperm, if mated, the male sperm exert dominance by displacing the smaller and slower hermaphrodite sperm from the spermatheca (Singson, 2001). Sperm competition can take place in the absence of fertilization, provided that mutant male sperm are motile and capable of reaching the spermatheca (Singson et al., 1999). Therefore, if males with motile, but fertilization-defective sperm, are mated to hermaphrodites, the self-fertility in hermaphrodites should be suppressed. We found that *trp-3*(*sy693*) males elicited a strong suppression on hermaphrodite self-fertility (Figures 4J and 4K). After 24 hr of mating with *trp-3*(*sy693*) males, each hermaphrodite only had an average of 21 self-progeny, approximately 15% of unmated hermaphrodites (Figure 4J). In contrast, hermaphrodites mated with *fer-1*(*hc1*) or *fer-15*(*hc15*) males, two mutants that only make immotile sperm, sired a similar number of self-progeny to that of unmated controls (Figure 4J). The suppression effect was not due to a reduction of the ovulation rate since the total ovulation events between mated and unmated hermaphrodites were similar (Figure 4L).

After mating with *trp-3* males, hermaphrodites were partially sterilized and laid many unfertilized oocytes, explaining why fertility was reduced while the rate of ovulation remained unchanged. These observations indicate that *trp-3* male sperm are not only motile, but also move vigorously enough to displace the endogenous hermaphrodite sperm from the spermatheca; yet they cannot fertilize oocytes, leading to a dominant-negative effect on fertilization. Also, about 5% of unfertilized oocytes dissected from *trp-3* uteri had sperm bound (Figure 4M; n = 300).

Taken together, it appears that the sterile phenotype

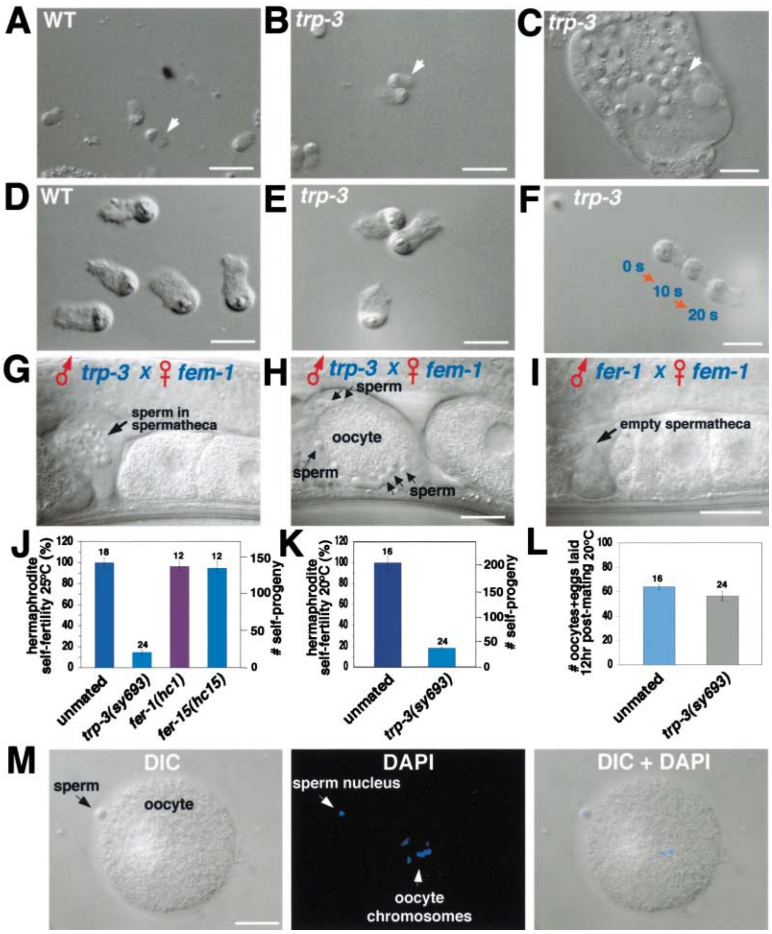

Figure 4. *trp-3*(*sy693*) Sperm Are Motile, but Fertilization Defective

(A) Dissected wild-type (*him-5*) hermaphrodite sperm. The arrow points to the pseudopod with villar projections on the surface. The scale bar in (A)–(C) = 10 μm.

(B) Dissected *trp-3*(*sy693*)*; him-5* hermaphrodite sperm show wild-type morphology. The arrow points to the pseudopod with villar projections on its surface.

(C) A dissected *trp-3*(*sy693*)*; him-5* hermaphrodite spermatheca with many sperm housed inside. The arrow points to a sperm's pseudopod with villar projections on the surface, indicative of wild-type morphology in situ.

(D) Wild-type (*him-5*) male mature sperm. Male spermatids were dissected from the gonad and activated with pronase. The scale bar in (D)–(F) = 5 μm.

(E) *trp-3*(*sy693*)*; him-5* male mature sperm showing wild-type morphology.

(F) *trp-3* mature sperm are motile in vitro. Shown is the superimposition of three time-lapse images acquired at 10 s intervals from a single *trp-3* mature sperm on a glass slide. Sperm were dissected from a *trp-3*(*sy694*)*; him-5* male and activated with pronase. The positions of the sperm at each time point are indicated on the side.

(G) *trp-3* sperm are motile in vivo. *trp-3*(*sy693*)*; him-5* males were crossed to *fem-1*(*hc17*) females at 25°C. The female spermathecae were then examined for the presence of *trp-3* sperm. The arrow points to the *trp-3* sperm that have migrated to the spermatheca. Scale bar = 20 μm.

(H) *trp-3*(*sy693*) sperm contact the oocyte during ovulation. Shown is an oocyte in a *fem-1*(*hc17*) female that had been mated with *trp-3*(*sy693*) males. The oocyte is wrapped in the spermatheca and surrounded by many *trp-3*(*sy693*) sperm. Arrows point to sperm. Scale bar = 10 μm.

(I) Immotile sperm cannot reach the spermatheca after mating. *fer-1*(*hc1*)*; him-5* or *fer15*(*hc15*)*; him-5* males were mated to *fem-1*(*hc17*) females under the same conditions as described in (G). No sperm were found in the female spermathecae. Data for *fer-15* are not shown. Scale bar = 20 μm.

(J) *trp-3*(*sy693*) male sperm efficiently suppress hermaphrodite self-fertility in a sperm competition assay. Assays were conducted at 25°C, the restricted temperature for *fer-1*(*hc1*) and *fer15*(*hc15*). Males were mated to *unc-24*(*e138*) hermaphrodites. The post-mating self-progeny laid by the hermaphrodites were counted. The number of progeny laid by unmated hermaphrodites after the first 24 hr was normalized to 100%. The Y-axis on the left indicates normalized self-fertility, while the Y-axis on the right indicates the total number of self-progeny laid post-mating. The error bars indicate SEM.

(K) *trp-3* male sperm efficiently suppress hermaphrodite self-fertility in a sperm competition assay at 20°C. The experiments were performed as described in (J), except that *unc-31*(*e169*) hermaphrodites were used.

(L) The suppression of hermaphrodite self-fertility by *trp-3* male sperm is not due to a reduced ovulation rate. The mated or unmated hermaphrodites in (L) were transferred to fresh plates every 4 hr for a total of 12 hr. The total number of eggs and oocytes laid during this period were counted and averaged.

(M) Adhesion of *trp-3* sperm to the oocyte. Unfertilized oocytes were dissected from the uterus of *trp-3*(*sy693*) hermaphrodites, fixed, mounted in DAPI, and then examined to look for sperm bound to the side or the top (~5%; n = 300). Coverslips were gently pushed down to slightly displace the specimen to examine adhesion. No such event was seen in *fer-15*(*hc15*) (n > 200). Shown in the left, middle, and right panel are a DIC image, DAPI image, and a superimposed DIC/DAPI image, respectively. Sperm were identified by the unique appearance of their nuclei and morphology. Scale bar = 10 mm.

in *trp-3* is caused by a sperm defect that is manifested after sperm contact the oocyte and before fertilization. Thus, *trp-3* seems to regulate sperm-egg interactions during fertilization.

Two Types of Calcium-Permeable Channels in *C. elegans* Sperm

We next sought to determine the mechanistic defect responsible for the inability of *trp*-3 sperm to fertilize the oocyte. The potential for TRP-3 to function as a calcium channel suggests that the *trp-3* defect might occur at the level of calcium signaling in sperm.

As is the case with mammalian sperm (Ren et al., 2001), *C. elegans* mature sperm are also refractory to patch-clamp recordings (Machaca et al., 1996). Therefore, we developed protocols to employ calcium-imaging techniques on *C. elegans* sperm, and observed two types of calcium-permeable channels in mature sperm. One channel appeared to be constitutively active, opening immediately upon introduction of extracellular calcium (Figures 5A and 5B). We refer to this channel as CAC (constitutively active calcium-permeable channel). The other channel was regulated by the state of calcium stores. After depletion of calcium stores with ionomycin

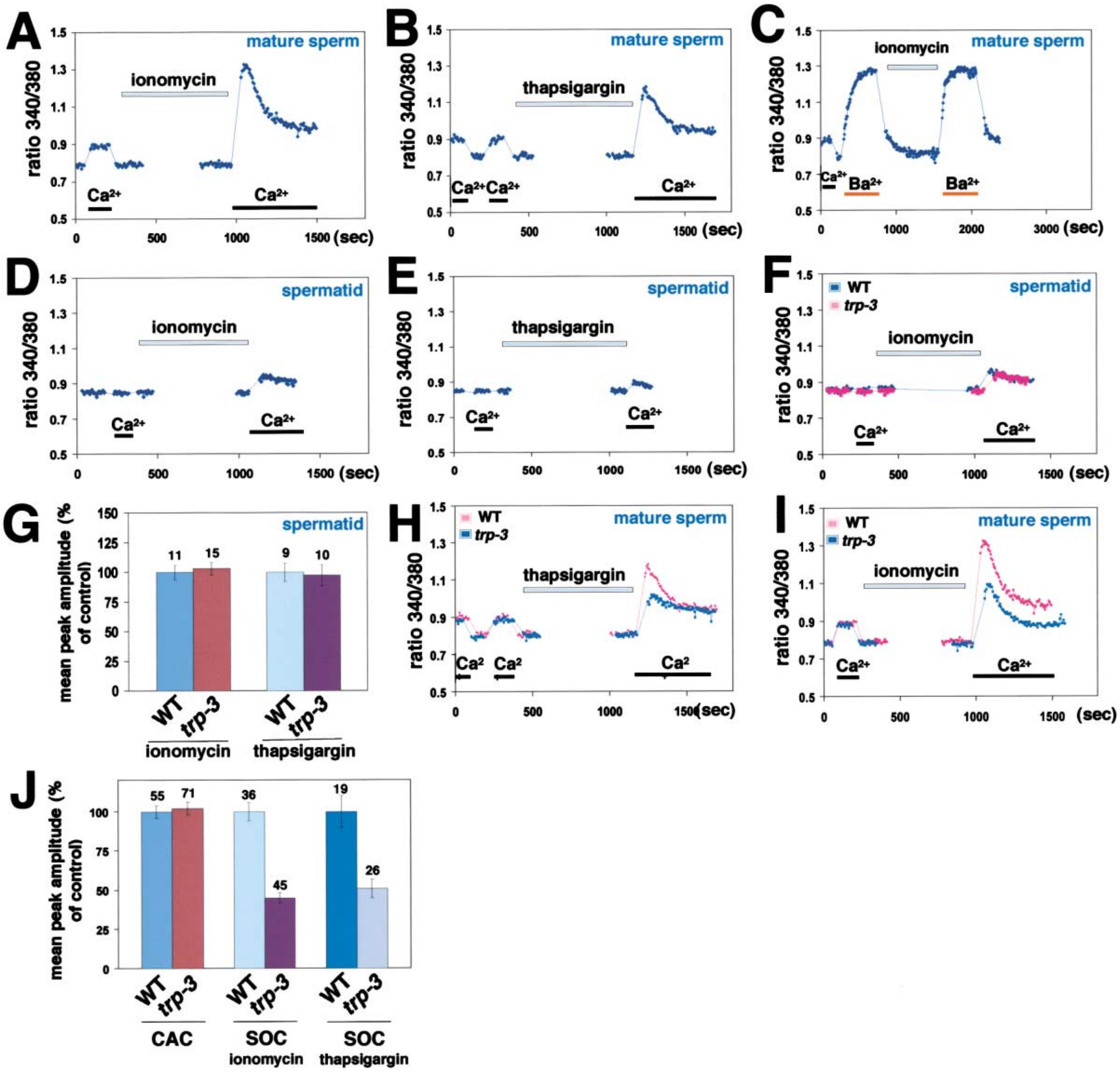

Figure 5. SOCE Is Markedly Reduced in *trp-3* Mature Sperm, but Not in *trp-3* Spermatids

(A and B) Wild-type mature sperm express at least two types of calcium influx channels. Shown is the average trace from all the sperm (~80) in a representative experiment. The duration of calcium application, ionomycin (0.5 μM) treatment (A) or thapsigargin (2 μM) treatment (B) is indicated. Traces are broken during ionomycin or thapsigargin treatment due to the pause of data acquisition to conserve disk space. No change in calcium level was observed during this period.

(C) CAC and SOC channels in mature sperm display distinct permeability to Ba^{2+}.

(D–E) Spermatids exhibit a much lower SOCE activity than do mature sperm.

(F) SOCE activities in *trp-3*(*sy693*) and wild-type spermatids are similar. The wild-type trace is a duplicate from (D).

(G) Histogram of mean peak SOC amplitudes in wild-type and *trp-3*(*sy693*) spermatids. The total number of independent recordings is indicated at the top of each column. The error bars represent SEM.

(H and I) Both the ionomycin- and thapsigargin-induced SOCE in *trp-3*(*sy693*) mature sperm are markedly reduced. The wild-type trace in (H) and (I) is a duplicate from (B) and (A), respectively.

(J) Histogram of mean peak CAC and SOCE activities in wild-type and *trp-3*(*sy693*) mature sperm. The SOC-dependent activity was calculated by subtracting the mean CAC amplitude from the peak amplitude activated by ionomycin or thapsigargin.

or thapsigargin in the absence of extracellular calcium, reapplication of calcium to the bath solution induced a much larger calcium influx that quickly inactivated and gradually declined to the baseline, characteristic of store-operated calcium entry (SOCE) (Figures 5A and 5B). We did not detect a large calcium release, presumably due to the small physical size (~3 μm) and the limited amount of intracellular organelles in nematode sperm. Nevertheless, we do not exclude the occurrence of a rapid calcium transient with short duration that might have eluded our detection. A similar treatment also fails to induce large calcium release in mouse sperm (O'Toole et al., 2000).

The SOC (store-operated channel) and CAC channels displayed different activities in Ba^{2+} and Ca^{2+} solutions. After switching to Ba^{2+}, a much larger (~5-fold increase) CAC amplitude developed (Figure 5C, n = 6). However, later treatment with ionomycin or thapsigargin failed to further increase the amplitude of the Ba^{2+} influx, suggesting that SOC has very limited activity in Ba^{2+} solution

(Figure 5C, n = 6). This effect was not due to an inhibition of SOCE by prior Ba^{2+} treatment because a similar amplitude was observed without prior Ba^{2+} incubation (data not shown). Attempts to test the effects of La^{3+} and Gd^{3+} were unsuccessful because of their toxicity to mature sperm (n = 4). We have also tested OAG, linolenic acid, arachidonic acid, Br-cAMP, and Br-cGMP, and found that none of these chemicals elicited significant calcium influx in mature sperm (n = 5). We note that in mouse sperm there also exist two distinct calcium channels, LVA (low-voltage-activated calcium channel) and SOC (O'Toole et al., 2000; Primakoff and Myles, 2002). We have no evidence whether CAC represents a type of LVA. Remarkably, when spermatids were assayed, a much lower SOCE activity was detected than that in mature sperm, and very little CAC activity was found in spermatids (Figures 5D and 5E).

SOCE Was Markedly Reduced in *trp-3* Mature Sperm, but Not in Spermatids

We next compared SOCE in *trp-3*(*sy693*) and wild-type spermatids, and found no significant difference with either ionomycin or thapsigargin treatment (Figures 5F and 5G). This observation is consistent with our finding that the *trp-3* defect was in the mature sperm but not in the spermatid. We found that *trp-3*(*sy693*) mature sperm exhibited much lower SOCE activity than did wild-type mature sperm. The mean amplitude induced by thapsigargin and ionomycin was reduced by 51% (Figures 5H and 5J, $p < 0.005$) and by 55% (Figures 5I and 5J, $p < 0.001$), respectively. In contrast, the CAC activity in *trp-3*(*sy693*) mature sperm was similar to that in wild-type (Figures 5H and 5J), indicating that the observed difference in SOCE was not due to a nonspecific defect in general calcium signaling. We would not expect a complete loss of SOCE in *trp-3*(*sy693*) mature sperm since *trp-3*(*sy693*) males still retained ~10% fertility. The ~50% reduction in SOCE in *trp-3* mature sperm was likely an underestimate, because we did not take into account the SOCE activity present in spermatids, which was clearly TRP-3 independent and probably contributed to the total SOCE activity in mature sperm (Figures 5F and 5G). Other *trp* genes such as *trp-1* and *trp-2* might account for the remaining SOCE activity in *trp-3* mutant sperm, and the residual fertility in *trp-3* mutant animals. Taken together, these data indicate that TRP-3 is necessary for the full SOCE activity in mature sperm, and suggest that the defect in SOCE in mature sperm might contribute to the inability of *trp-3*(*sy693*) sperm to fertilize oocytes.

Expression of TRP-3 in 293 Cells Enhanced Calcium Entry

To test whether TRP-3 is sufficient to promote SOCE in vitro, we expressed TRP-3 in 293 cells. As is the case with most mammalian cell lines, 293 cells exhibited endogenous SOCE (Figures 6A and 6C). Despite this high endogenous activity, expression of TRP-3 augmented both the ionomycin- and thapsigargin-dependent calcium influx by 64% and 61%, respectively (Figures 6A–6D, $p < 0.005$; Figure 6G, $p < 0.005$).

As some TRPC proteins can be activated by both store-operated and receptor-operated mechanisms (reviewed in Putney et al., 2001; Venkatachalam et al., 2002). We tested whether TRP-3 can also be activated through stimulation of the Gq/11-PLCβ pathway by coexpressing TRP-3 and H1R, a histamine receptor known to be coupled to Gq/11 (Hofmann et al., 1999). Histamine induced a large calcium release in the absence of extracellular calcium, but reintroduction of calcium only elicited a small calcium influx in cells transfected with H1R alone. In contrast, a much larger calcium influx (5.1 fold, $p < 0.001$) developed if cells were cotransfected with H1R and TRP-3 (Figures 5E, 5F, and 5H), suggesting that stimulation of Gq/11-PLCβ activates TRP-3. The TRP-3 dependent activities in 293 cells were sensitive to La^{3+} (91 ± 6% inhibition at 100 μM for thapsigargin, n = 5; 92 ± 7% for histamine, n = 4) and Gd^{3+} (94 ± 8% inhibition at 100 μM for thapsigargin, n = 5; 89 ± 11% for histamine, n = 4). As we observed in mature sperm (Figure 5C), the TRP-3-dependent activity stimulated by either thapsigargin/ionomycin or histamine in 293 cells was also minimal in Ba^{2+} solution (data not shown). Since TRPC channels heteromultimerize in vivo as well as interact with endogenous TRP subunits and signaling pathways in heterologous systems, it is difficult to compare the in vivo and in vitro activities of TRPC channels (reviewed in Venkatachalam et al., 2002). Nevertheless, our results demonstrate that expression of TRP-3 in 293 cells is sufficient to promote calcium influx, presumably by forming a channel or by interacting with endogenous signaling machinery.

Translocation of TRP-3 from Intracellular Vesicles to the Plasma Membrane during Sperm Activation

We wondered why mature sperm exhibited a much higher SOCE activity than did spermatids (Figures 5A, 5B, 5D, and 5E). One explanation is that the proteins mediating SOCE such as TRP-3 are not expressed in spermatids. We think this unlikely since there is no gene transcription or protein translation during sperm activation (spermiogenesis) (L'Hernault, 1997). Thus, any TRP-3 protein in mature sperm must also be present in spermatids. We therefore asked whether TRP-3 protein localization was altered during sperm activation. Shown in Figure 7 are confocal images of anti-TRP-3 immunostaining performed on spermatids and mature sperm. TRP-3 did not display surface staining in spermatids; instead, it seemed to be localized to discrete intracellular vesicles (Figure 7A). This staining was not seen in *trp-3*(*sy693*) mutants (Figures 7D–7F), indicating that the antibody was specific. Preincubation with the peptide antigen also blocked TRP-3 staining in wild-type sperm (data not shown). One major class of intracellular vesicles present in spermatids is the ER/Golgi derived vesicles, called membranous organelles (MOs) (L'Hernault, 1997). Expression of TRP-3 overlapped with an MO marker, 1CB4 (Okamoto and Thomson, 1985), indicating that TRP-3 was enriched in the MOs of spermatids (Figures 7B and 7C). ICB4 also detected a ring-like structure that outlined the MO vesicles. This signal was likely nonspecific because it does not appear in immuno-gold staining (Okamoto and Thomson, 1985). TRP-3 did not overlap with this nonspecific signal (Figure 7C).

During sperm activation, the MO vesicles fuse with

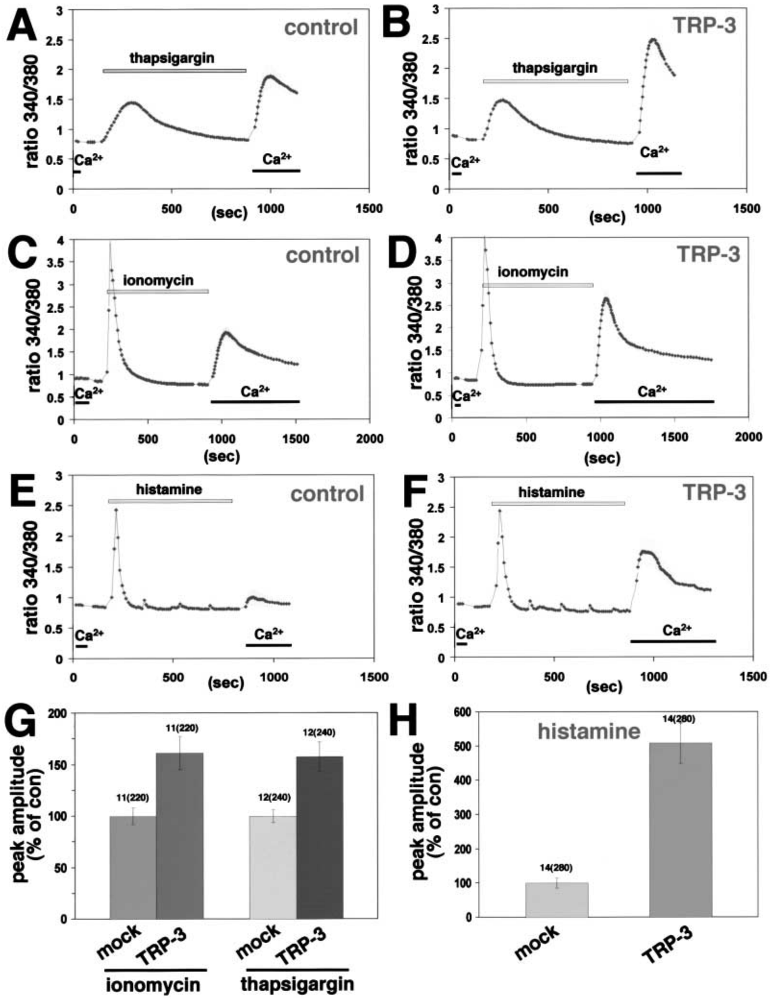

Figure 6. Expression of TRP-3 in 293 Cells Promotes Calcium Influx

(A and B) Expression of TRP-3 in 293 cells promotes thapsigargin-induced SOCE. An empty pIRES2-EGFP vector (A) or a plasmid encoding *trp-3* cDNA (B) was transfected into 293 cells. Shown is the trace averaged from 20 selected GFP-positive cells in a representative experiment. The error bars represent SEM. The duration of calcium application and thapsigargin treatment (2 μM) is indicated.

(C and D) Expression of TRP-3 in 293 cells promotes ionomycin-induced SOCE. The experiments were performed as described in (A and B). 0.5 μM ionomycin was used to deplete intracellular calcium stores.

(E and F) Stimulation of Gq/11-PLCβ activates TRP-3 in 293 cells. A plasmid encoding H1R was cotransfected with the empty pIRES2-EGFP vector or with a plasmid encoding *trp-3* into 293 cells. The stores were depleted with histamine (1 mM).

(G) Histogram of mean peak SOC amplitude activated by ionomycin and thapsigargin. The total number of independent recordings is indicated at the top of each column. 20 GFP positive cells from each recording were randomly selected for analysis.

(H) Histogram of mean peak amplitude stimulated by histamine.

the plasma membrane, which is accompanied by the development of a pseudopod (depicted in Figure 7P) (L'Hernault, 1997). The fused MO vesicles remain connected to the plasma membrane in the cell body via permanent fusion pores, and thus their lumen are exposed to the cell's exterior (depicted in Figure 7P) (L'Hernault, 1997). Therefore, the fused MO membranes are in fact part of the plasma membrane in the cell body of mature sperm. Based on the fate of the MOs during sperm activation, the MO-localized TRP-3 would become a plasma-membrane-protein after the MOs fuse with the plasma membrane during sperm activation. This is indeed what we have observed (Figures 7G–7I and Supplemental Figures S1A–S1D [available online at http://www.cell.com/cgi/content/full/114/3/285/DC1]). Interestingly, unlike the fused MOs that were restricted to the cell body and were excluded from the pseudopod, TRP-3 staining was also present in the pseudopod (Figures 7G–7I and Supplemental Figure S1D). The observation that TRP-3 and the fused MOs exhibited a largely nonoverlapping pattern suggests that TRP-3 proteins likely diffuse out of the fused MOs and translocate to the rest of the cell membrane including the pseudopod during sperm activation.

We next sought to provide further evidence for the translocation model. We reasoned that if TRP-3 is initially localized to the MOs and later translocates to the plasma membrane, then blocking fusion of the MOs with the plasma membrane during sperm activation should prevent TRP-3 translocation. To test this, we took advantage of the *fer-1*(*hc1*) mutant, in which the MOs fail to fuse with the plasma membrane even though sperm activation proceeds (Achanzar and Ward, 1997). As predicted, in *fer-1*(*hc1*) mature sperm, the TRP-3 signal was arrested in discrete intracellular vesicles and continued to colocalize with the MO marker, indicating that TRP-3 did not translocate to the plasma membrane (Figures 7M–7O). As a result, TRP-3 was excluded from the pseudopod in *fer-1*(*hc1*) mature sperm ([H] in Supplemental Figure S1). Taken together, our data indicate that TRP-3 is stored in intracellular vesicles in spermatids and translocates to the plasma membrane during sperm activation. Since this translocation coincides with a marked increase in SOCE (Figures 5A, 5B, 5D, and 5E), it provides an in vivo mechanism for the regulation of TRP-3 activity. As expected, we failed to detect such an increase in SOCE in *fer-1* mature sperm (Figures S1I–S1J). The lack of TRP-3 protein in the spermatid plasma membrane is also consistent with our observation that the defect in SOCE was only detected in

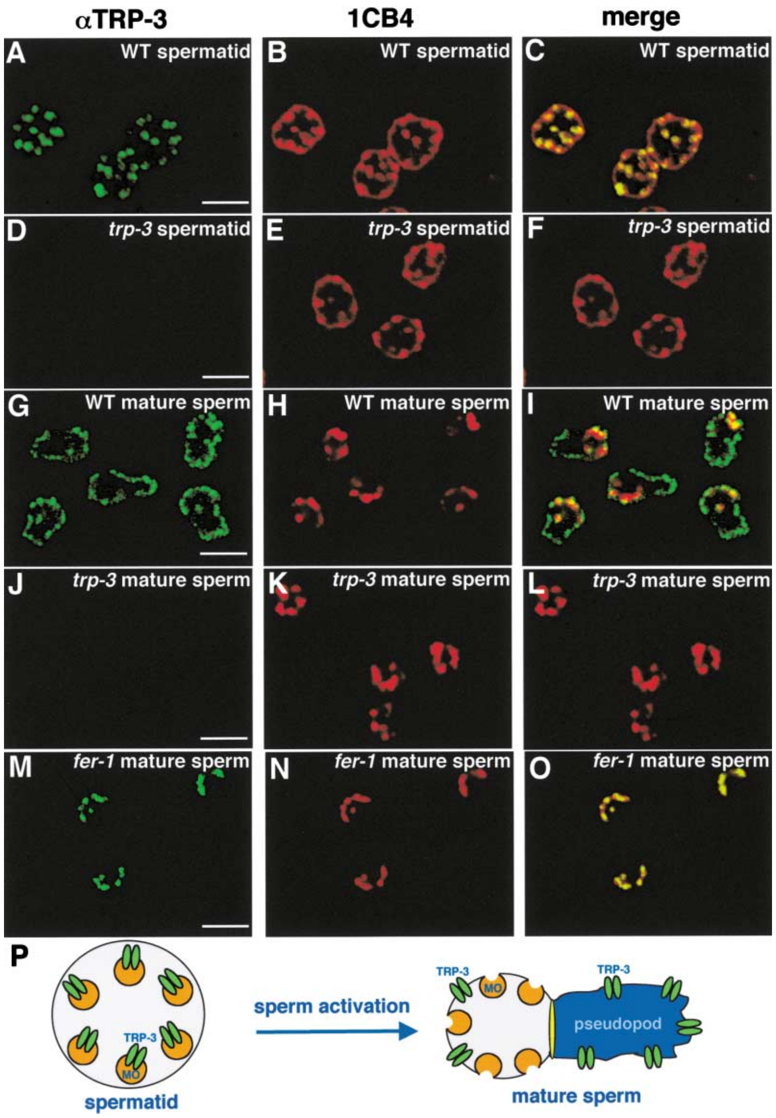

Figure 7. Translocation of TRP-3 Protein during Sperm Activation

(A–O) Shown are confocal images of immunostaining performed on spermatids or mature sperm. Genotypes are indicated in each image. All the images in the left column were stained with anti-TRP3, while the ones in the middle column were stained with 1CB4, a marker for the MO vesicles. The images in the right column are merged images of anti-TRP3 and 1CB4 staining. Scale bar = 3 μm.

(A–C) TRP-3 is localized to discrete intracellular vesicles in wild-type (*him-5*) spermatids and colocalizes with 1CB4, a marker for the MO vesicles.

(D–F) The TRP-3 antibody does not detect a signal in *trp-3*(*sy693*); *him-5* spermatids.

(G–I) TRP-3 is localized near the plasma membrane in wild-type mature sperm and exhibits a distinct staining pattern from the MO vesicles. Note that TRP-3 is present in both the cell body and the pseudopod, whereas the MOs are absent in the pseudopod and restricted to the cell body. See Supplemental Figure S1 (available at http://www.cell.com/cgi/content/full/114/3/285/DC1) for DIC images.

(J–L) No TRP-3 signal is detected in *trp-3*(*sy693*); *him-5* mature sperm.

(M–O) TRP-3 is arrested in intracellular vesicles in *fer-1*(*hc1*) mature sperm and colocalizes with the MO vesicles. See the Supplemental Figure S1 for DIC images. Note that both TRP-3 and the MOs are absent in the pseudopod in *fer-1*(*hc1*) sperm.

(P) A schematic model showing TRP-3 translocation during sperm activation (spermiogenesis). The round red circles depict the MO vesicles, while the green ovals represent TRP-3. The pseudopod is labeled in blue while the laminar membrane is labeled in yellow.

trp-3 mature sperm, but not in spermatids (Figures 5F and 5G).

Discussion

TRP-3 Is Required for Sperm-Egg Interactions during Fertilization

To explore the biological functions of TRPC proteins, we identified a sperm-enriched *C. elegans TRPC* homolog, *trp-3*, and demonstrated that it was required for fertilization. Furthermore, we identified an in vivo mechanism for the regulation of TRP-3 activity, namely its subcellular translocation.

Several lines of evidence indicate that the sterile phenotype in *trp-3* mutants results from a defect in sperm. First, we have determined that ovulation and oocyte maturation in *trp-3* mutants are similar to those in wild-type. Second, wild-type sperm, but not seminal fluid, rescue the sterile phenotype in *trp-3* mutants. Third, the expression pattern of TRP-3 protein is consistent with the sperm defect. We have further demonstrated that *trp-3* mutant sperm are motile and are capable of mediating gamete contact with oocytes. As *C. elegans* oocytes lack egg coats, these observations indicate that the inability of *trp-3* sperm to fertilize oocytes results from a defect in sperm-oocyte plasma membrane interactions.

TRPCs Might Regulate Gamete Fusion during Fertilization

Unlike mammalian sperm, *C. elegans* sperm do not possess an acrosome, possibly because of the lack of egg coats in *C. elegans* oocytes, which renders the acrosome reaction unnecessary in sperm. During nematode fertilization, following gamete contact are likely the processes of gamete binding and fusion. We have demonstrated that the *trp-3* defect is manifested at a step after gamete contact. Is sperm-oocyte binding defective in *trp-3* mutants? In contrast to mammals, in which sperm-oocyte binding and fusion can readily take place in vitro, nematode sperm-oocyte interactions occur only within the spermatheca, making it difficult to address such a question. We did observe a small percentage of oocytes dissected from *trp-3* uteri bound with sperm, consistent with *trp-3* sperm being capable of mediating gamete binding. This observation raises the possibility that the *trp-3* defect might be at the level of gamete fusion. The majority of dissected oocytes did not have sperm bound, which might have been caused by an immediate decrease in the affinity of sperm-egg binding in the uterus as such binding would not have been favored outside of the spermatheca. In mammals, calcium has been found to be required for sperm-oocyte fusion, but not for binding of sperm and egg-coat-free oocytes (Yanagimachi, 1978), consistent with our hypothesis. Another possibility is that there might be two phases of sperm-oocyte binding, weak followed by tight binding; if so, *trp-3* mutant sperm might be defective in mediating the tight binding with oocytes.

Are the functions of TRPC proteins conserved in fertilization? The possibility that mammalian TRPCs might play a role in sperm-egg plasma membrane interactions has largely escaped attention, because most efforts thus far have been directed toward identifying a role for TRPCs in the sperm acrosome reaction and motility. For example, a mouse TRPC2 antibody has been found to suppress the acrosome reaction in vitro (Jungnickel et al., 2001), supporting a role for mTRPC2 in the acrosome reaction in vivo. It has also been proposed that TRPCs might play a role in sperm motility (Castellano et al., 2003). However, in vivo evidence is still lacking for such roles for TRPCs in fertility. In fact, both TRPC2 and TRPC4 knockout mice are fertile, and no fertility defect has been reported, although a defect in pheromone sensation and in agonist-induced vasorelaxation and lung microvascular permeability increases has been detected in TRPC2 and TRPC4 mutant mice, respectively (Freichel et al., 2001; Leypold et al., 2002; Stowers et al., 2002; Tiruppathi et al., 2002). It is not clear whether other mouse TRPCs might play a role in the sperm acrosome reaction and motility. If the function of TRPC proteins is conserved in fertilization, it might occur at a step that is common to both nematode and mammalian fertilization. In light of our data on TRP-3 and the fact that there is no acrosome reaction in nematode fertilization, we propose that TRPCs might regulate gamete fusion in mammals.

Besides TRPC2 and TRPC4, other TRPC homologs are also expressed in mouse sperm. For example, mouse TRPC6 has been reported to be expressed in the posterior part of the sperm head (Castellano et al., 2003). Since the membranes in this region are involved in mediating gamete binding and fusion, but are not implicated in the acrosome reaction (Yanagimachi, 1994), we speculate that TRPC proteins located here might play a role in later steps of fertilization including gamete fusion. It would be interesting to see whether any TRPC knockout mice exhibit a defect in these processes.

We propose that during sperm-egg interactions, binding of sperm receptors and their oocyte ligand(s) in the plasma membrane might signal the opening of TRPC channels in sperm, and the ensuing calcium influx would then trigger a series of signaling events culminating in gamete fusion.

In mammals, sustained calcium influx is also required for other cell-cell fusion events such as myoblast fusion (Shainberg et al., 1969). However, the calcium channel(s) underlying this process remains elusive (Bernheim and Bader, 2002; Park et al., 2002). It has been demonstrated that AVP (arginine-vasopressin), an agonist to the Gq/11-PLCβ pathway, is a potent inducer of the fusion of myogenic cells (Teti et al., 1993). As TRPC proteins reside downstream of the Gq/11-PLCβ pathway (Zhu et al., 1996), it is possible that AVP acts, at least in part, by activating these channels.

Mechanisms that Regulate TRP-3 Activity

The signaling pathway(s) leading to the activation of TRPCs remains highly controversial (Putney et al., 2001; Venkatachalam et al., 2002). Several models have been proposed, including store-depletion, receptor-activation, and vesicle fusion/secretion (Venkatachalam et al., 2002). Despite the fact that expression of TRP-3 in 293 cells enhances SOCE, TRP-3 expression seems to promote receptor-operated calcium entry (ROCE) much more efficiently in these cells. One explanation is that TRP-3 is activated in a receptor-operated manner during sperm-egg interactions, and that the observed effect on SOCE might result from a functional interaction between TRP-3 and the endogenous signaling machinery that activates SOCE. Nonetheless, our results demonstrate that loss of TRP-3 in sperm results in a defect in calcium influx, which is associated with the inability of *trp-3* sperm to fertilize oocytes.

We have found that TRP-3 translocates from intracellular vesicles to the plasma membrane via vesicle fusion during sperm activation. A similar phenomenon has been observed with TRPV2 and TRPL (Bahner et al., 2002; Kanzaki et al., 1999). While this fusion/translocation provides a mechanism for TRP-3 regulation, it is not clear whether such a mechanism would play a more direct role in the activation of TRP-3. Nevertheless, the focus of the current study is to identify the biological functions of TRPC proteins in vivo, and future studies are needed to further address the mechanisms for TRPC activation. With the isolation of these *trp-3* null alleles and the ease of *C. elegans* genetics, in principle, we should be able to generate reduction-of-function *trp-3* alleles that would allow us to perform unbiased genetic screens for suppressors and enhancers to identify components of TRPC signaling pathway(s) in vivo.

Experimental Procedures

Genetics

All the strains carried *him-5*(*e1490*) unless otherwise specified. *trp-3* deletions were isolated as described (Jansen et al., 1997). Deletions were backcrossed to *him-5*(*e1490*) once and then to N2 seven times. *him-5*(*e1490*) was kept during backcrossing. The *him-5*(*e1490*) strain was also backcrossed to N2 three times before phenotypic analyses. *sur-5::gfp* was used as the transformation marker to make *trp-3*(*sy693*)*; him-5; Ex[C03D4*+*sur-5::gfp]*. C03D4 is a cosmid containing the full-length *trp-3* gene (information from WormBase).

Phenotypic Analyses

Hermaphrodite fertility was determined by counting all the progeny sired by hermaphrodites over 96 hr starting at the L4 stage. Male fertility was determined by mating L4 males with L4 hermaphrodites or females at a 3:2 ratio for 24 hr at 20°C or 25°C; the cross progeny sired by hermaphrodites or females over 96 hr was counted.

The sperm competition assay was performed as follows. L4 males were mated with L4 hermaphrodites at a 4:1 ratio for 24 hr at 20°C or 25°C. Post-mating hermaphrodite self-progeny sired over the next 72 hr were counted. The progeny laid during the mating period were not counted due to the difficulty of determining the timing of mating.

To examine the ovulation cycle, oocyte maturation, fertilization, and early embryogenesis, worms were anesthetized wtih 0.1% tricaine + 0.01% tetramisole and recorded with time-lapse video (McCarter et al., 1999). For egg staining, eggs mechanically released from the hermaphrodite uterus were subjected to a quick freeze/thaw cycle with liquid N_2, fixed in 4°C methanol for 20 min, and then mounted in DAPI for microscopy.

Cell Culture and Transfection

293 cells were cultured in MEM (10% FBS, 1 mM pyruvate, penicillin/streptomycin in 5% CO_2) at 37°C. Subconfluent cells were transfected with Fugene 6 (Roche) according to the manufacturer's instructions.

Antibody Production and Purification

A synthetic peptide corresponding to residues 801–822 (DAGTKVAPKDDKPQNNPVLART) in TRP-3 was conjugated with KLH and injected into rabbits. Affinity purification was performed with a SulfoLink kit (Pierce) according to the manufacturer's instructions.

Immunofluorescence and Calcium Imaging

See Supplemental Data available online at http://www.cell.com/cgi/content/full/114/3/285/DC1.

Acknowledgments

We thank B. Perry for help with deletion libraries, X. Dong and J. DeModena for assistance on confocal microscopy, A. Coulson for the cosmid, Y. Kohara for EST clones, and A Singson for 1CB4 antibodies. We also thank P. Wes, G. Schindelman, N. Moghal, A. Singson, and C. Montell for critical comments on the manuscript, and H. Florman for helpful discussions. Some strains were obtained from the Caenorhabditis Genetics Center. This work was supported by the HHMI, with which P.W.S. is an Investigator. X.-Z.S.X. is supported by a Helen Hay Whitney Foundation Fellowship.

Received: April 30, 2003
Revised: June 23, 2003
Accepted: July 11, 2003
Published: August 7, 2003

References

Achanzar, W.E., and Ward, S. (1997). A nematode gene required for sperm vesicle fusion. J. Cell Sci. *110*, 1073–1081.

Bahner, M., Frechter, S., Da Silva, N., Minke, B., Paulsen, R., and Huber, A. (2002). Light-regulated subcellular translocation of Drosophila TRPL channels induces long-term adaptation and modifies the light-induced current. Neuron *34*, 83–93.

Bernheim, L., and Bader, C.R. (2002). Human myoblast differentiation: Ca(2+) channels are activated by K(+) channels. News Physiol. Sci. *17*, 22–26.

Browning, H., and Strome, S. (1996). A sperm-supplied factor required for embryogenesis in C. elegans. Development *122*, 391–404.

Castellano, L.E., Trevino, C.L., Rodriguez, D., Serrano, C.J., Pacheco, J., Tsutsumi, V., Felix, R., and Darszon, A. (2003). Transient receptor potential (TRPC) channels in human sperm: expression, cellular localization and involvement in the regulation of flagellar motility. FEBS Lett. *541*, 69–74.

Caterina, M.J., and Julius, D. (2001). The vanilloid receptor: a molecular gateway to the pain pathway. Annu. Rev. Neurosci. *24*, 487–517.

Freichel, M., Suh, S.H., Pfeifer, A., Schweig, U., Trost, C., Weissgerber, P., Biel, M., Philipp, S., Freise, D., Droogmans, G., et al. (2001). Lack of an endothelial store-operated Ca2+ current impairs agonist-dependent vasorelaxation in TRP4−/− mice. Nat. Cell Biol. *3*, 121–127.

Harteneck, C., Plant, T.D., and Schultz, G. (2000). From worm to man: three subfamilies of TRP channels. Trends Neurosci. *23*, 159–166.

Hofmann, T., Obukhov, A.G., Schaefer, M., Harteneck, C., Gudermann, T., and Schultz, G. (1999). Direct activation of human TRPC6 and TRPC3 channels by diacylglycerol. Nature *397*, 259–263.

Jansen, G., Hazendonk, E., Thijssen, K.L., and Plasterk, R.H. (1997). Reverse genetics by chemical mutagenesis in Caenorhabditis elegans. Nat. Genet. *17*, 119–121.

Jungnickel, M.K., Marrero, H., Birnbaumer, L., Lemos, J.R., and Florman, H.M. (2001). Trp2 regulates entry of Ca2+ into mouse sperm triggered by egg ZP3. Nat. Cell Biol. *3*, 499–502.

Kanzaki, M., Zhang, Y.Q., Mashima, H., Li, L., Shibata, H., and Kojima, I. (1999). Translocation of a calcium-permeable cation channel induced by insulin-like growth factor-I. Nat. Cell Biol. *1*, 165–170.

Kelly, W.G., and Fire, A. (1998). Chromatin silencing and the maintenance of a functional germline in Caenorhabditis elegans. Development *125*, 2451–2456.

Leypold, B.G., Yu, C.R., Leinders-Zufall, T., Kim, M.M., Zufall, F., and Axel, R. (2002). Altered sexual and social behaviors in trp2 mutant mice. Proc. Natl. Acad. Sci. USA *99*, 6376–6381.

L'Hernault, S. (1997). Spermatogenesis. In *C elegans* II (New York: Cold Spring Harbor Laboratory Press), pp. 271–294.

L'Hernault, S.W., Shakes, D.C., and Ward, S. (1988). Developmental genetics of chromosome I spermatogenesis-defective mutants in the nematode Caenorhabditis elegans. Genetics *120*, 435–452.

Machaca, K., DeFelice, L.J., and L'Hernault, S.W. (1996). A novel chloride channel localizes to Caenorhabditis elegans spermatids and chloride channel blockers induce spermatid differentiation. Dev. Biol. *176*, 1–16.

McCarter, J., Bartlett, B., Dang, T., and Schedl, T. (1999). On the control of oocyte meiotic maturation and ovulation in Caenorhabditis elegans. Dev. Biol. *205*, 111–128.

Montell, C., Birnbaumer, L., and Flockerzi, V. (2002a). The TRP channels, a remarkably functional family. Cell *108*, 595–598.

Montell, C., Birnbaumer, L., Flockerzi, V., Bindels, R.J., Bruford, E.A., Caterina, M.J., Clapham, D.E., Harteneck, C., Heller, S., Julius, D., et al. (2002b). A unified nomenclature for the superfamily of TRP cation channels. Mol. Cell *9*, 229–231.

Okamoto, H., and Thomson, J.N. (1985). Monoclonal antibodies which distinguish certain classes of neuronal and supporting cells in the nervous tissue of the nematode Caenorhabditis elegans. J. Neurosci. *5*, 643–653.

O'Toole, C.M., Arnoult, C., Darszon, A., Steinhardt, R.A., and Florman, H.M. (2000). Ca(2+) entry through store-operated channels in mouse sperm is initiated by egg ZP3 and drives the acrosome reaction. Mol. Biol. Cell *11*, 1571–1584.

Park, J.Y., Lee, D., Maeng, J.U., Koh, D.S., and Kim, K. (2002). Hyperpolarization, but not depolarization, increases intracellular Ca(2+) level in cultured chick myoblasts. Biochem. Biophys. Res. Commun. *290*, 1176–1182.

Primakoff, P., and Myles, D.G. (2002). Penetration, adhesion, and fusion in mammalian sperm-egg interaction. Science *296*, 2183–2185.

Putney, J.W., Jr., Broad, L.M., Braun, F.J., Lievremont, J.P., and Bird, G.S. (2001). Mechanisms of capacitative calcium entry. J. Cell Sci. *114*, 2223–2229.

Reinke, V., Smith, H.E., Nance, J., Wang, J., Van Doren, C., Begley, R., Jones, S.J., Davis, E.B., Scherer, S., Ward, S., and Kim, S.K. (2000). A global profile of germline gene expression in C. elegans. Mol. Cell *6*, 605–616.

Ren, D., Navarro, B., Perez, G., Jackson, A.C., Hsu, S., Shi, Q., Tilly, J.L., and Clapham, D.E. (2001). A sperm ion channel required for sperm motility and male fertility. Nature *413*, 603–609.

Shainberg, A., Yagil, G., and Yaffe, D. (1969). Control of myogenesis in vitro by Ca 2 + concentration in nutritional medium. Exp. Cell Res. *58*, 163–167.

Singson, A. (2001). Every sperm is sacred: fertilization in Caenorhabditis elegans. Dev. Biol. *230*, 101–109.

Singson, A., Mercer, K.B., and L'Hernault, S.W. (1998). The C. elegans spe-9 gene encodes a sperm transmembrane protein that contains EGF-like repeats and is required for fertilization. Cell *93*, 71–79.

Singson, A., Hill, K.L., and L'Hernault, S.W. (1999). Sperm competition in the absence of fertilization in Caenorhabditis elegans. Genetics *152*, 201–208.

Spence, A.M., Coulson, A., and Hodgkin, J. (1990). The product of fem-1, a nematode sex-determining gene, contains a motif found in cell cycle control proteins and receptors for cell-cell interactions. Cell *60*, 981–990.

Stowers, L., Holy, T.E., Meister, M., Dulac, C., and Koentges, G. (2002). Loss of sex discrimination and male-male aggression in mice deficient for TRP2. Science *295*, 1493–1500.

Teti, A., Naro, F., Molinaro, M., and Adamo, S. (1993). Transduction of arginine vasopressin signal in skeletal myogenic cells. Am. J. Physiol. *265*, C113–C121.

Tiruppathi, C., Freichel, M., Vogel, S.M., Paria, B.C., Mehta, D., Flockerzi, V., and Malik, A.B. (2002). Impairment of store-operated Ca2+ entry in TRPC4(−/−) mice interferes with increase in lung microvascular permeability. Circ. Res. *91*, 70–76.

Tobin, D., Madsen, D., Kahn-Kirby, A., Peckol, E., Moulder, G., Barstead, R., Maricq, A., and Bargmann, C. (2002). Combinatorial expression of TRPV channel proteins defines their sensory functions and subcellular localization in C. elegans neurons. Neuron *35*, 307–318.

Venkatachalam, K., van Rossum, D.B., Patterson, R.L., Ma, H.T., and Gill, D.L. (2002). The cellular and molecular basis of store-operated calcium entry. Nat. Cell Biol. *4*, E263–E272.

Wassarman, P.M. (1999). Mammalian fertilization: molecular aspects of gamete adhesion, exocytosis, and fusion. Cell *96*, 175–183.

Yanagimachi, R. (1978). Calcium requirement for sperm-egg fusion in mammals. Biol. Reprod. *19*, 949–958.

Yanagimachi, R. (1994). Mammalian fertilization. In The Physiology of Reproduction (New York: Raven Press), pp. 189–317.

Zhu, X., Jiang, M., Peyton, M., Boulay, G., Hurst, R., Stefani, E., and Birnbaumer, L. (1996). trp, a novel mammalian gene family essential for agonist-activated capacitative Ca2+ entry. Cell *85*, 661–671.

Accession Numbers

The GenBank Accession number for the *trp-3* cDNA is AY342006.